

Polymer size in dilute solutions in the good-solvent regime

Sergio Caracciolo, Bortolo Matteo Mognetti

Dipartimento di Fisica and INFN – Sezione di Milano I Università degli Studi di Milano

Via Celoria 16, I-20133 Milano, Italy

e-mail: Sergio.Caracciolo@sns.it, Bortolo.Mognetti@mi.infn.it

Andrea Pelissetto

Dipartimento di Fisica and INFN – Sezione di Roma I

Università degli Studi di Roma “La Sapienza”

P.le A. Moro 2, I-00185 Roma, Italy

e-mail: Andrea.Pelissetto@roma1.infn.it

Abstract

We determine the density expansion of the radius of gyration, of the hydrodynamic radius, and of the end-to-end distance for a monodisperse polymer solution in good-solvent conditions. We consider the scaling limit (large degree of polymerization), including the leading scaling corrections. Using the expected large-concentration behavior, we extrapolate these low-density expansions outside the dilute regime, obtaining a prediction for the radii for any concentration in the semidilute region. For the radius of gyration, comparison with field-theoretical predictions shows that the relative error should be at most 5% in the limit of very large polymer concentrations.

PACS: 61.25.Hq, 82.35.Lr

I. INTRODUCTION

For sufficiently high molecular weights, dilute and semidilute polymer solutions under good-solvent conditions exhibit a universal scaling behavior, as predicted by the renormalization group.^{1–5} For instance, if R is some typical dimension of the polymer, then $R \approx aN^\nu$, where N is the degree of polymerization, a is a constant that depends on density, temperature, and chemical details, and ν a universal exponent, $\nu \approx 0.5876$ (Ref. 6). From an experimental point of view, two quantities R are easily accessible in the dilute regime. The radius of gyration R_g is determined in small-angle scattering experiments. For small wave numbers q , the static form factor behaves as

$$F(q) = \frac{1}{N^2} \sum_{\alpha\beta} \langle e^{i\mathbf{q} \cdot (\mathbf{r}_\alpha - \mathbf{r}_\beta)} \rangle \approx 1 - \frac{q^2}{3} R_g^2 + O(q^4), \quad (1.1)$$

that allows the determination of R_g . The second quantity of interest is the hydrodynamic radius R_H , which is related to the chain diffusion constant D that can be measured in inelastic scattering experiments:⁷

$$D = \frac{k_B T}{6\pi\eta R_H}, \quad (1.2)$$

where η is the viscosity. In theoretical work, another quantity is often used, the end-to-end distance R_e , which can, in principle, be accessible in experiments with polymers with tagged endpoints.⁴

In this paper we consider the density dependence of these three quantities. In general, if R is one of the quantities defined above or any functions of them, in the dilute regime we can write

$$R(c) = \hat{R}[1 + R_1 c + R_2 c^2 + O(c^3)], \quad (1.3)$$

where c is the polymer number density and $\hat{R} \equiv R(c = 0)$. The coefficients R_1 , R_2 , etc. depend on chemical details. However, as $N \rightarrow \infty$ the ratios $S_n \equiv R_n / \hat{R}_g^{3n}$ approach universal constants S_n^* that are independent of temperature—as long as the polymer is in the good-solvent regime—and chemical properties. Thus, if N is large (scaling regime) we can write the universal expression

$$\frac{R(c)}{\hat{R}} = 1 + S_1^* c \hat{R}_g^3 + S_2^* (c \hat{R}_g^3)^2 + O[(c \hat{R}_g^3)^3]. \quad (1.4)$$

In many cases, polymers are not long enough to be in the scaling regime and thus it is important to include scaling corrections. As predicted by the renormalization group and extensively verified numerically, for N large but finite we have for the expansion coefficients of quantities related to the end-to-end distance and to the radius of gyration

$$S_n = \frac{R_n}{\hat{R}_g^{3n}} \approx S_n^* (1 + k_2 s_n N^{-\Delta}), \quad (1.5)$$

where Δ is a universal exponent whose best estimate is⁸ $\Delta = 0.515 \pm 0.007_{-0.000}^{+0.010}$. The constants S_n^* and s_n are universal. The constant k_2 encodes all chemical details and nonuniversal properties of the solution—temperature, for instance. It can be determined by considering the scaling corrections to some renormalization-group invariant polymer quantity. We use the interpenetration radius Ψ that can be determined from the osmotic pressure and represents one of the most easily experimentally accessible quantities.⁹ In the large- N limit it behaves as

$$\Psi \approx \Psi^* (1 + k_2 N^{-\Delta}). \quad (1.6)$$

This relation defines the constant k_2 . The constant Ψ^* is universal and known with very good precision:¹⁰ $\Psi^* = 0.24693 \pm 0.00013$. Other estimates are reported in Ref. 11. Universal ratios related to the hydrodynamic radius scale differently because of the presence of corrections proportional to $N^{1-\nu}$ (Ref. 12). Note finally that, given two different quantities R_1 and R_2 that characterize the polymer size, their zero-density ratio \hat{R}_1/\hat{R}_2 approaches a universal constant \hat{R}_{12}^* for $N \rightarrow \infty$.

For the purpose of determining the universal constants defined above we perform a Monte Carlo simulation of the lattice Domb-Joyce model,¹³ considering walks of length varying between 100 and 8000 and three different penalties for the self-intersections. We are able to obtain the leading density correction with a relative precision of 0.5% for R_g and R_e and of 5% for R_H . We also estimate the second density correction, although with limited precision.

These results show that density corrections are very small below the overlap concentration $c^* \equiv 3/(4\pi\hat{R}_g^3)$, and that a simple approximation that assumes a linear dependence on the density works quite well up to $c \approx c^*$. Once the virial expansion is known, we can try to resum it to obtain an interpolation formula that is valid in the whole semidilute regime. In Ref. 10 we have shown that a simple extrapolation of the virial expansion for the osmotic pressure that takes into account the expected large-concentration behavior works reasonably well. Comparison with experimental data and with other theoretical predictions shows that the error is less than 1% in the dilute region and rises at most to 5-10% deep in the semidilute regime. We use here the same strategy for the radii, determining simple expressions that reproduce the virial expansion for $c \rightarrow 0$ and have the correct large-density behavior. Comparison with other theoretical results shows that, at least for R_g , the interpolation formula has an error of at most 5%.

The paper is organized as follows. In Sec. II we derive the virial expansion for a generic quantity that depends on the structure of a single polymer, like the radii defined above. In Sec. III we define the model and the quantities we compute. In Sec. IV we analyze the Monte Carlo results. In Sec. V we present our conclusions and compare our results with those obtained in other approaches.

II. VIRIAL EXPANSION FOR SINGLE-POLYMER PROPERTIES

We wish now to derive the density expansion of $R(c)$, where R is a single-polymer property. We consider L polymers in a volume V with configurational partition function

$$Q_L = \int d\mu \exp \left(-\beta \sum_{i < j} V_{ij}^{\text{inter}} \right) \quad (2.1)$$

$$d\mu \equiv \left[\prod_{i\alpha} d^3 \mathbf{x}_{\alpha i} \right] \exp \left(-\beta \sum_i V_i^{\text{intra}} \right), \quad (2.2)$$

where V_{ij}^{inter} is the sum of all terms of the Hamiltonian that correspond to interactions of monomers belonging to two different polymers i and j , V_i^{intra} is the contribution due

to interactions of monomers belonging to the same polymer i , and $\mathbf{x}_{\alpha i}$ is the position of monomer α belonging to polymer i . As usual, we define the Mayer function

$$f_{ij} \equiv \exp(-\beta V_{ij}^{\text{inter}}) - 1. \quad (2.3)$$

Since R is a single-polymer property, we can assume that it depends only on the coordinates $\mathbf{x}_{\alpha 1}$ of the monomers of the first polymer. Thus, we wish to compute the expansion of

$$\langle R \rangle = \frac{1}{Q_L} \int d\mu R(\{\mathbf{x}_{\alpha 1}\}) \exp \left(-\beta \sum_{i < j} V_{ij}^{\text{inter}} \right), \quad (2.4)$$

for $c \rightarrow 0$. The term linear in the number density $c \equiv L/V$ is easily derived:

$$\frac{Q_L}{Q_{0,L}} \langle R \rangle = \langle R \rangle_0 + \binom{L-1}{2} \langle R f_{23} \rangle_0 + (L-1) \langle R f_{12} \rangle_0 + \dots \quad (2.5)$$

$$\frac{Q_L}{Q_{0,L}} = 1 + \binom{L}{2} \langle f_{12} \rangle_0 + \dots \quad (2.6)$$

where

$$Q_{0,L} \equiv \int d\mu \quad \langle \mathcal{O} \rangle_0 \equiv \frac{1}{Q_{0,L}} \int d\mu \mathcal{O}. \quad (2.7)$$

It follows that, for $L, V \rightarrow \infty$ at fixed concentration, we have

$$\langle R \rangle = \hat{R} + c \left[J_1(R) - \hat{R} I_2 \right], \quad (2.8)$$

where \hat{R} is the zero-density value of R , and

$$I_2 \equiv \int d^3 \mathbf{r}_{12} \langle f_{12} \rangle_{\mathbf{0}, \mathbf{r}_{12}}, \quad (2.9)$$

$$J_1(R) \equiv \int d^3 \mathbf{r}_{12} \langle R f_{12} \rangle_{\mathbf{0}, \mathbf{r}_{12}}. \quad (2.10)$$

Here $\langle \cdot \rangle_{\mathbf{0}, \mathbf{r}}$ indicates an average over two independent polymers such that the first one starts at the origin and the second starts in \mathbf{r} . In the mean values R is a function of the coordinates of the first walk.

The correction of order c^2 can be worked out analogously. We define

$$I_3 \equiv \int d^3\mathbf{r}_{12} d^3\mathbf{r}_{13} \langle f_{12} f_{13} f_{23} \rangle_{\mathbf{0}, \mathbf{r}_{12}, \mathbf{r}_{13}} \quad (2.11)$$

$$T_1 \equiv \int d^3\mathbf{r}_{12} d^3\mathbf{r}_{13} \langle f_{12} f_{13} \rangle_{\mathbf{0}, \mathbf{r}_{12}, \mathbf{r}_{13}} - \left[\int d^3\mathbf{r}_{12} \langle f_{12} \rangle_{\mathbf{0}, \mathbf{r}_{12}} \right]^2 \quad (2.12)$$

$$J_2(R) \equiv \int d^3\mathbf{r}_{12} d^3\mathbf{r}_{13} \langle R f_{12} f_{13} \rangle_{\mathbf{0}, \mathbf{r}_{12}, \mathbf{r}_{13}} \quad (2.13)$$

$$J_3(R) \equiv \int d^3\mathbf{r}_{12} d^3\mathbf{r}_{13} \langle R f_{12} f_{23} \rangle_{\mathbf{0}, \mathbf{r}_{12}, \mathbf{r}_{13}} \quad (2.14)$$

$$J_4(R) \equiv \int d^3\mathbf{r}_{12} d^3\mathbf{r}_{13} \langle R f_{12} f_{13} f_{23} \rangle_{\mathbf{0}, \mathbf{r}_{12}, \mathbf{r}_{13}} , \quad (2.15)$$

where $\langle \cdot \rangle_{\mathbf{0}, \mathbf{r}_2, \mathbf{r}_3}$ refers to averages over three polymers, the first one starting in the origin, the second in \mathbf{r}_2 , etc. We obtain finally

$$\begin{aligned} \langle R \rangle = & \hat{R} + c \left[J_1(R) - \hat{R} I_2 \right] + \\ & \frac{1}{2} c^2 \left[J_2(R) + 2J_3(R) + J_4(R) - 3\hat{R} T_1 - \hat{R} I_3 - 4I_2 J_1(R) + \hat{R} I_2^2 \right] + O(c^3). \end{aligned} \quad (2.16)$$

In the following we shall consider a lattice model for polymers. In this case, the previous expressions must be trivially modified, replacing each integral with the corresponding sum over all lattice points.

III. MODEL AND OBSERVABLES

Since we are interested in computing universal quantities, we can use any model that captures the basic polymer properties. For computational convenience we shall consider a lattice model. A polymer of length N is modelled by a random walk $\{\mathbf{r}_0, \mathbf{r}_1, \dots, \mathbf{r}_N\}$ with $|\mathbf{r}_\alpha - \mathbf{r}_{\alpha+1}| = 1$ on a cubic lattice. To each walk we associate a Boltzmann factor

$$e^{-\beta H} = e^{-w\sigma}, \quad \sigma = \sum_{0 \leq \alpha < \beta \leq N} \delta_{\mathbf{r}_\alpha, \mathbf{r}_\beta}, \quad (3.1)$$

with $w > 0$. The factor σ counts how many self-intersections are present in the walk. This model is similar to the standard self-avoiding walk (SAW) model in which polymers are modelled by random walks in which self-intersections are forbidden. The SAW model is obtained for $w = +\infty$. For finite positive w self-intersections are possible although energetically penalized. For any positive w , this model—hereafter we will refer to it as Domb-Joyce (DJ)

model—has the same scaling limit of the SAW model¹³ and thus allows us to compute the universal scaling functions that are relevant for polymer solutions. The DJ model has been extensively studied numerically in Ref. 8. There, it was also shown that there is a particular value of w , w^* , for which corrections to scaling with exponent Δ vanish: the nonuniversal constant k_2 is zero for this particular value of w . Thus, simulations at $w = w^*$ are particularly convenient since the scaling limit can be observed for smaller values of N . In Ref. 8 w^* was shown to be approximately equal to 0.505838 ($e^{-w^*} = 0.603$), while in Ref. 10 it was found $w^* \approx 0.47 \pm 0.02$.

The DJ model can be efficiently simulated by using the pivot algorithm.^{14–17} For the SAW an efficient implementation is discussed in Ref. 18. The extension to the DJ model is straightforward, the changes in energy being taken into account by means of Metropolis test. Such a step should be included carefully in order not to loose the good scaling behavior of the CPU time for attempted move. We use here the implementation discussed in Ref. 19.

We shall be interested in the quantities that characterize the size of the polymer and have been defined in the introduction. In the lattice model they are defined as follows:

$$R_g^2 = \frac{1}{2(N+1)^2} \left\langle \sum_{\alpha\beta} (\mathbf{r}_\alpha - \mathbf{r}_\beta)^2 \right\rangle, \quad (3.2)$$

$$\frac{1}{R_H} = \frac{1}{(N+1)^2} \left\langle \sum_{\alpha\beta: \mathbf{r}_\alpha \neq \mathbf{r}_\beta} \frac{1}{|\mathbf{r}_\alpha - \mathbf{r}_\beta|} \right\rangle, \quad (3.3)$$

$$R_e^2 = \langle (\mathbf{r}_0 - \mathbf{r}_N)^2 \rangle. \quad (3.4)$$

The expansion coefficients S_n have been determined by using the expressions reported in Sec. II with

$$f_{ij} = e^{-\beta V_{ij}} - 1 = e^{-w\sigma_{ij}} - 1 \quad (3.5)$$

$$\sigma_{ij} = \sum_{\alpha\beta} \delta_{\mathbf{r}_{\alpha i}, \mathbf{r}_{\beta j}}. \quad (3.6)$$

Here $\mathbf{r}_{\alpha i}$ is the position of monomer α of polymer i . To compute the corresponding lattice sums, we use a simple generalization of the hit-or-miss algorithm discussed in Ref. 20 and in the appendix of Ref. 10.

In the dilute limit we write

$$\frac{R_g^2}{\hat{R}_g^2} = 1 + S_{1,g}(c\hat{R}_g^3) + S_{2,g}(c\hat{R}_g^3)^2 + \dots \quad (3.7)$$

$$\frac{R_e^2}{\hat{R}_e^2} = 1 + S_{1,e}(c\hat{R}_g^3) + S_{2,e}(c\hat{R}_g^3)^2 + \dots \quad (3.8)$$

The coefficients $S_{n,\#}$ have a finite limit for $N \rightarrow \infty$. Including the leading scaling correction, in the scaling limit they behave as follows:

$$S_{n,\#}(N) = S_{n,\#}^* \left(1 + \frac{k_2 s_{n,\#}}{N^\Delta} + \dots \right), \quad (3.9)$$

where the constants $S_{n,\#}^*$ and $s_{n,\#}$ are universal. The factor k_2 depends instead on chemical details, temperature, etc. and is fixed by the large- N behavior (1.6) of the interpenetration radius Ψ .⁹

Beside the coefficients parametrizing the density dependence of the radii, we can also consider the large- N behavior of the radii that we parametrize as

$$\hat{R}_g^2 = a_g N^{2\nu} (1 + k_2 r_g N^{-\Delta} + \dots), \quad (3.10)$$

$$\hat{R}_e^2 = a_e N^{2\nu} (1 + k_2 r_e N^{-\Delta} + \dots). \quad (3.11)$$

The constants r_g and r_e are universal as well as the ratio $A_{ge}^* \equiv a_g/a_e$. This quantity can also be determined directly by considering

$$A_{ge} = \frac{\hat{R}_g^2}{\hat{R}_e^2} \approx A_{ge}^* (1 + k_2 r_{ge} N^{-\Delta} + \dots), \quad (3.12)$$

where $r_{ge} = r_g - r_e$.

Quantities involving the hydrodynamic radius must be analyzed differently, due to the appearance of new nonuniversal corrections proportional to $N^{\nu-1}$. For instance, as discussed in Ref. 12, $1/\hat{R}_H$, which is the quantity measured in MC calculations, scales as

$$\frac{1}{\hat{R}_H} = \frac{\alpha_1}{N^\nu} (1 + a_1 N^{-\Delta}) + \frac{b}{N} + \dots = \frac{\alpha_1}{N^\nu} \left(1 + \frac{b}{\alpha_1} N^{\nu-1} + a_1 N^{-\Delta} + \dots \right). \quad (3.13)$$

The analytic term gives rise to a new correction proportional to $N^{\nu-1} = N^{-0.412}$. It decays slower than the standard one proportional to $N^{-\Delta} = N^{-0.5}$ and does not satisfy any universality property. We also consider the density expansion

$$\frac{\hat{R}_H}{R_H} = 1 + S_{1,H}(c\hat{R}_g^3) + S_{2,H}(c\hat{R}_g^3)^2 + \dots \quad (3.14)$$

and the ratio

$$A_{gH} \equiv \frac{\hat{R}_g}{\hat{R}_H}. \quad (3.15)$$

For $N \rightarrow \infty$, $S_{n,H}$ and $A_{g,H}$ converge to universal constant $S_{n,H}^*$ and A_{gH}^* . Note that it is more convenient to consider \hat{R}_g/\hat{R}_H than \hat{R}_H/\hat{R}_g , since the latter quantity has additional corrections proportional to $N^{2\nu-2} = N^{-0.825}$, etc.

IV. ANALYSIS OF THE MONTE CARLO DATA

We have performed three sets of simulations at $w = 0.375, 0.505838, 0.775$, using walks with $100 \leq N \leq 8000$. Results are reported in Tables I, II, III, and IV. The numerical data that concern R_g^2 and R_e^2 have been analyzed as discussed in Refs. 21, 10. Therefore, if $Q = A_{ge}, S_{1,g}, S_{2,g}, S_{1,e}$, and $S_{2,e}$, we fit the data to

$$Q(N, w) \approx Q^* + \frac{a_Q(w)}{N^\Delta} + \frac{c_Q(w)}{N^{\Delta_{2,\text{eff}}}}. \quad (4.1)$$

For Δ we use the best available estimate: $\Delta = 0.515 \pm 0.007_{-0.000}^{+0.010}$ (Ref. 8). The term $1/N^{\Delta_{2,\text{eff}}}$ should take into account analytic corrections behaving as $1/N$, and nonanalytic ones of the form $N^{-2\Delta}$, $N^{-\Delta_2}$ (Δ_2 is the next-to-leading correction-to-scaling exponent). As discussed in Ref. 21, one can lump all these terms into a single one with exponent $\Delta_{2,\text{eff}} = 1.0 \pm 0.1$. The results are reported in Table V. The reported error is the sum of the statistical error and of the systematic one due to the uncertainty on Δ and $\Delta_{2,\text{eff}}$. In order to detect additional corrections to scaling we have repeated the fit several times, including each time only the data with $N \geq N_{\text{min}}$. More precise estimates can be obtained by using the universality of the ratios of the correction-to-scaling amplitudes. As we did in Ref. 10, we can simultaneously analyze two quantities Q_1 and Q_2 , using the fact that $a_{Q_1}(w) = r_{12}a_{Q_2}(w)$, with r_{12} independent of w . Thus, one can fit simultaneously all data for Q_1 and Q_2 , taking as free parameters Q_1^* , Q_2^* , $a_{Q_1}(w_i)$, $c_{Q_1}(w_i)$, $c_{Q_2}(w_i)$, and r_{12} . We have reanalyzed the data for $S_{1,g}, S_{2,g}, S_{1,e}$, and

$S_{2,e}$ using this method, taking always as second variable \hat{R}_g^2/\hat{R}_e^2 . The results are reported in Table VI. The improvement is quite significant, the errors decreasing by a factor of 2-3. We do not observe significant residual scaling corrections and take the result with $N_{\min} = 500$ as our final estimate. Therefore

$$A_{ge}^* = 0.15988 \pm 0.00004, \quad (4.2)$$

$$S_{1,g}^* = -0.3152 \pm 0.0007, \quad (4.3)$$

$$S_{2,g}^* = -0.087 \pm 0.005, \quad (4.4)$$

$$S_{1,e}^* = -0.3853 \pm 0.0007, \quad (4.5)$$

$$S_{2,e}^* = -0.027 \pm 0.006. \quad (4.6)$$

Note that all density corrections are negative—this is not surprising since, by increasing the density, the polymer size decreases. Moreover, both for R_g^2 and R_e^2 , the second density correction is significantly smaller than the first one. There are in the literature several estimates of A_{ge}^* (see Ref. 11 for an extensive list of references). The most precise ones are: $A_{ge}^* = 0.1599 \pm 0.0002$ (Ref. 20) and $A_{ge}^* = 0.15995 \pm 0.00010$ (Ref. 22). They are both in good agreement with our result. We can also compare the estimates of $S_{1,g}^*$ and $S_{2,g}^*$ with those obtained by using one-loop perturbation theory:^{5,23} $S_{1,g}^* \approx -1.19$ and $S_{2,g}^* \approx 5.74$. They both significantly differ from our estimates, indicating that the perturbative renormalization group is not accurate (at one-loop order) for these quantities.

In the analysis of quantities involving the hydrodynamic radius we should take into account the corrections proportional to $N^{\nu-1} = N^{-0.412}$. These new corrections are particularly strong and depend only slightly on w , as it can be seen from the results in Tables I, IV: for all values of w , \hat{R}_g/\hat{R}_H and $S_{n,H}$ show the same monotonic behavior, indicating that corrections proportional to $N^{-\Delta}$ are much smaller than those proportional to $N^{\nu-1}$ (remember that the $N^{-\Delta}$ corrections approximately vanish for $w = 0.505838$ and have opposite sign in the other two cases). In order to determine the scaling-limit value of A_{gH} , $S_{1,H}$, and $S_{2,H}$ we fit the data to

$$Q(N, w) = Q^* + \frac{a(w)}{N^{1-\nu}} + \frac{c(w)}{N^\Delta} . \quad (4.7)$$

Results are reported in Table V for several values of N_{\min} . As before, the error takes into account the uncertainty on ν and Δ . In all cases, the results show small trends with N_{\min} indicating that there are some small additional scaling corrections that are not taken into account by the fit Ansatz (4.7). We quote as our final results:

$$A_{gH}^* = 1.5810 \pm 0.0010 \quad (4.8)$$

$$S_{1,H}^* = 0.082 \pm 0.004 \quad (4.9)$$

$$S_{2,H}^* = 0.050 \pm 0.020. \quad (4.10)$$

The error should be large enough to take into account all residual systematic corrections. Note that also in this case density corrections are small. The result for A_{gH}^* is in good agreement with that obtained in Ref. 12: $A_{gH}^* = 1.591 \pm 0.007$.

Finally, we compute the universal scaling-correction coefficients: our data are precise enough to provide estimates of $s_{1,g}$, $s_{1,e}$, r_{ge} , r_e , and r_g . The first three quantities can be determined as discussed in Ref. 21. If $Q(N, w)$ is a renormalization-group invariant quantity we consider

$$T_Q(N) \equiv \frac{\Psi^*}{Q^*} \left[\frac{Q(N, w_1) - Q(N, w_2)}{\Psi(N, w_1) - \Psi(N, w_2)} \right], \quad (4.11)$$

which should converge asymptotically to the correction-to-scaling amplitude with corrections of order $N^{-\Delta_{\text{eff}}}$, with $\Delta_{\text{eff}} = 0.5 \pm 0.1$. In practice we use the data with $w_1 = 0.375$ and $w_2 = 0.775$ and fit $T_Q(N)$ to

$$T_Q(N) = a + bN^{-\Delta_{\text{eff}}}. \quad (4.12)$$

We find that the correction-to-scaling coefficients are quite small:

$$r_{ge} = -0.0040 \pm 0.0004, \quad (4.13)$$

$$s_{1,g} = -0.050 \pm 0.010, \quad (4.14)$$

$$s_{1,e} = -0.050 \pm 0.020. \quad (4.15)$$

As for $s_{2,g}$ and $s_{2,e}$ we only obtain upper bounds: $s_{2,g} = -0.1 \pm 0.2$, $|s_{2,e}| \lesssim 0.2$. In order to determine r_e and r_g we first define $Q_R(N) \equiv \hat{R}^2(2N)/\hat{R}^2(N)$ and then

$$T_R(N) \equiv \frac{2^{-2\nu}\Psi^*}{1-2^\Delta} \left[\frac{Q_R(N, w_1) - Q_R(N, w_2)}{\Psi(2N, w_1) - \Psi(2N, w_2)} \right] \quad (4.16)$$

that converges to r_e or r_g , depending on the radius one is considering, with corrections of order $N^{-\Delta_{\text{eff}}}$. We obtain:

$$r_g = -0.36 \pm 0.07, \quad (4.17)$$

$$r_e = -0.28 \pm 0.08. \quad (4.18)$$

Finally, if we analyze as before the quantity

$$T_{R_g, R_e}(N) \equiv \frac{Q_{R_g}(N, w_1) - Q_{R_g}(N, w_2)}{Q_{R_e}(N, w_1) - Q_{R_e}(N, w_2)}, \quad (4.19)$$

we obtain a direct estimate of r_g/r_e :

$$r_g/r_e = 1.2 \pm 0.3. \quad (4.20)$$

This is consistent with the estimate

$$\frac{r_g}{r_e} = 1 + \frac{r_{ge}}{r_e} = 1.014 \pm 0.004, \quad (4.21)$$

obtained by using r_{ge} and r_e . These results can be compared with those appearing in the literature. Ref. 24 gives $-0.5 \lesssim r_g \lesssim -0.4$ and $r_g/r_e = 1.25 \pm 0.04$, while Ref. 8 gives $r_e = -0.41 \pm 0.01$. The estimates of r_g and r_e are consistent with ours, while that for r_g/r_e differs significantly, given the small error bars.

V. CONCLUSIONS

The results of the previous Section allow us to determine the radii in the dilute regime. We find

$$\frac{R_g^2}{\hat{R}_g^2} = 1 - 0.0752\Phi_p - 0.0050\Phi_p^2 + \dots + k_\Phi(0.003\Phi_p + b_g\Phi_p^2 \dots), \quad (5.1)$$

$$\frac{R_e^2}{\hat{R}_e^2} = 1 - 0.0920\Phi_p - 0.0015\Phi_p^2 + \dots + k_\Phi(0.004\Phi_p + b_e\Phi_p^2 \dots), \quad (5.2)$$

$$\frac{\hat{R}_H}{R_H} = 1 + 0.0195\Phi_p + 0.003\Phi_p^2 + \dots, \quad (5.3)$$

where we have introduced the polymer packing fraction

$$\Phi_p \equiv \frac{4\pi\hat{R}_g^3}{3}c = \frac{4\pi\hat{R}_g^3}{3}\frac{N_A}{M}\rho, \quad (5.4)$$

N_A is the Avogadro number, M the molar mass of the polymer, c and ρ the number density and the ponderal concentration respectively. The constants b_g and b_e depend on $s_{2,g}$ and $s_{2,e}$ and thus we only have an upper bound: $|b_g| \lesssim 1 \cdot 10^{-3}$, $|b_e| \lesssim 2 \cdot 10^{-4}$. The constant k_Φ takes into account scaling corrections. It scales as $N^{-\Delta}$, where N is the degree of polymerization, and therefore vanishes in the scaling limit. It is defined by the small-density behavior of the osmotic pressure:¹⁰

$$Z = \frac{\beta\Pi}{c} \approx 1 + 1.313\Phi_p + 0.559\Phi_p^2 - 0.122\Phi_p^3 + \dots + k_\Phi(\Phi_p + 1.13\Phi_p^2 + \dots). \quad (5.5)$$

Expansions (5.1), (5.2), (5.3) are supposed to be valid up to $\Phi_p \approx 1$. In this range, the linear term in the density dominates, the next-to-leading term being quite small, at variance with the behavior of the osmotic pressure. Note also that the density dependence is very small in all cases. The nonuniversal parameter k_Φ allows us to take into account the deviations from the scaling limit due to the finite degree of polymerization (as long as scaling corrections are small). It can be obtained from measurements of the osmotic pressure by using Eq. (5.5). Once k_Φ is known, everything is fixed and the previous expressions give us the radii in the whole dilute regime $\Phi_p \lesssim 1$. Note that corrections to scaling in the radii are much smaller than in the osmotic pressure.

It is worthwhile to try to extrapolate the above-reported expansions outside the dilute regime. As in Ref. 10 we will use a simple interpolation formula that takes into account the large- Φ_p behavior of the radii. For $\Phi_p \rightarrow \infty$ we have⁵

$$\frac{R^2}{\hat{R}^2} \sim \Phi_p^{-(2\nu-1)/(3\nu-1)} \sim \Phi_p^{-0.230}, \quad (5.6)$$

which is a consequence of the fact that, at fixed nonvanishing monomer concentration, polymers behave as Gaussian coils as $N \rightarrow \infty$. It is easy to write down interpolation formulas that take into account Eq. (5.6) and reproduce the previous expansions for $\Phi_p \rightarrow \infty$:

$$\begin{aligned} \frac{R_g^2}{\hat{R}_g^2} &= (1 + 0.655\Phi_p + 0.28\Phi_p^2)^{-0.115}, \\ \frac{R_e^2}{\hat{R}_e^2} &= (1 + 0.801\Phi_p + 0.37\Phi_p^2)^{-0.115}, \\ \frac{\hat{R}_H}{R_H} &= (1 + 0.34\Phi_p + 0.10\Phi_p^2)^{0.0574}. \end{aligned} \quad (5.7)$$

We do not attempt to include also scaling corrections here, since we have only estimated one single coefficient. Of course, these expressions are very precise in the dilute limit. In order to assess their precision in the semidilute regime we can compare with field-theoretical estimates^{25–27,5} and with Monte Carlo results.²⁸ In Fig. 1 we compare expression (5.7) for the radius of gyration with the expression reported in Ref. 25. The two curves are quite close. They differ at most by 3.2% (for $\Phi_p \approx 1.5$) and, as $\Phi_p \rightarrow \infty$, they give $R_g^2/\hat{R}_g^2 \approx 1.18\Phi_p^{-0.230}$ (Ref. 25) and $R_g^2/\hat{R}_g^2 \approx 1.16\Phi_p^{-0.230}$ [Eq. (5.7)]. Note that the largest differences are observed for small values of Φ_p (for $\Phi_p = 0.4$ the curves differ by 2%) where our expression is by construction very accurate. This is related to the fact that, as observed in Sec. IV, the low-density coefficients for the radii are poorly determined by one-loop field-theoretical calculations. Similar results are obtained by using the expressions reported in Ref. 5. For instance, they predict $R_g^2/\hat{R}_g^2 \approx 1.14\Phi_p^{-0.230}$ [see Eq. (18.12) in Ref. 5]. In Fig. 1 we also report some Monte Carlo data taken from Ref. 28. They are somewhat lower (differences are less than 5%) than prediction (5.7) and in better agreement with the field-theoretical curve, but they could be affected by finite-size and scaling corrections. This comparison shows that our expression for the density dependence of R_g is reasonably accurate, the error being apparently less than 5% in the whole semidilute region. We are not aware of similar field-theoretical results for the other radii, so that we are unable to estimate the precision of the extrapolation for R_e and R_H .

The authors thank Tom Kennedy for providing his efficient simulation code for lattice self-avoiding walks.

REFERENCES

- ¹ de Gennes, P.G. *Phys. Lett.* **1972**, *38A*, 339.
- ² de Gennes, P.G. *Scaling Concepts in Polymer Physics*; Cornell University Press: Ithaca, NY, 1979.
- ³ Freed, K.F. *Renormalization Group Theory of Macromolecules*; Wiley: New York, 1987.
- ⁴ des Cloizeaux, J.; Jannink, G. *Polymers in Solution: Their Modelling and Structure*; Clarendon: Oxford, 1990.
- ⁵ Schäfer, L. *Excluded Volume Effects in Polymer Solutions*; Springer Verlag: Berlin, 1999.
- ⁶ At present the most accurate estimates of ν are $\nu = 0.58758 \pm 0.00007$ (Ref. 8), $\nu = 0.5874 \pm 0.0002$ [Prellberg, T. *J. Phys. A* **2001**, *34*, L599.], $\nu = 0.58765 \pm 0.00020$ [Hsu, H.-P.; Nadler, W.; Grassberger, P. *Macromolecules* **2004**, *37*, 4658.]. For an extensive list of results, see Ref. 11.
- ⁷ Doi M.; Edwards S. F. *The Theory of Polymer Dynamics*; Oxford University Press: Oxford, 1986.
- ⁸ Belohorec, P.; Nickel, B.G. “Accurate universal and two-parameter model results from a Monte-Carlo renormalization group study,” Guelph University report (1997), unpublished.
- ⁹ The interpenetration radius Ψ is determined from the low-density behavior of the osmotic pressure Π . If $\Pi/(RT\rho) = 1/M + B_2\rho + O(\rho^2)$ (M is the molar mass of the polymer, ρ the ponderal concentration, and T the absolute temperature), then we define $\Psi \equiv 2(4\pi)^{-3/2}M^2B_2R_g^{-3}/N_A$, where N_A is the Avogadro number.
- ¹⁰ Caracciolo, S.; Moggetti, B.M.; Pelissetto, A. “Virial coefficients and osmotic pressure in polymer solutions in good-solvent conditions,” available at www.arxiv.org/abs/cond-mat/0605535.
- ¹¹ Pelissetto, A.; Vicari, E. *Phys. Rept.* **2002**, *368*, 549.

- ¹² Dünweg, B.; Reith, D.; Steinhauser, M.; Kremer, K. *J. Chem. Phys.* **2002**, *117*, 914.
- ¹³ Domb, C.; Joyce, G.S. *J. Phys. C* **1972**, *5*, 956.
- ¹⁴ Lal, M. *Molec. Phys.* **1969**, *17*, 57.
- ¹⁵ MacDonald, B.; Jan, N.; Hunter, D.L.; Steinitz, M.O. *J. Phys. A: Math. Gen.* **1985**, *18*, 2627.
- ¹⁶ Madras, N.; Sokal, A.D. *J. Stat. Phys.* **1988**, *50*, 109.
- ¹⁷ Sokal, A.D. in *Monte Carlo and Molecular Dynamics Simulations in Polymer Science*, edited by K. Binder; Oxford Univ. Press: Oxford, 1995.
- ¹⁸ Kennedy, T. *J. Stat. Phys.* **2002**, *106*, 407.
- ¹⁹ Caracciolo, S.; Parisi, G.; Pelissetto, A. *J. Stat. Phys.* **1994**, *77*, 519.
- ²⁰ Li, B.; Madras, N.; Sokal, A.D. *J. Stat. Phys.* **1995**, *80*, 661.
- ²¹ Pelissetto, A.; Hansen, J.-P. *J. Chem. Phys.* **2005**, *122*, 134904.
- ²² Grassberger, P.; Sutter, P.; Schäfer, L. *J. Phys. A* **1997**, 7039.
- ²³ See Eq. (18.11) of Ref. 5. Note that \hat{s} is related to $c\hat{R}_g^3$ by $\Phi_p \equiv 4\pi c\hat{R}_g^3/3 = 1.169\hat{s}$.
- ²⁴ Nickel, B.G. *Macromolecules* **1991**, *24*, 1358.
- ²⁵ Ohta, T.; Nakanishi, A. *J. Phys. A* **1983**, *16*, 4155.
- ²⁶ Freed, K.F. *J. Chem. Phys.* **1983**, *79*, 6357.
- ²⁷ Schäfer, L. *Macromolecules* **1984**, *17*, 1357.
- ²⁸ Müller, M.; Binder, K.; Schäfer, L. *Macromolecules* **2000**, *33*, 4568.

TABLES

TABLE I. Estimates of the ratios $A_{ge} = \hat{R}_g^2/\hat{R}_e^2$ and $A_{gH} = \hat{R}_g/\hat{R}_H$.

N	$w = 0.375$	$w = 0.505838$	$w = 0.775$
A_{ge}			
100	0.161771(15)	0.1609797(95)	0.159965(14)
250	0.160842(15)	0.160283(11)	0.159637(10)
500	0.160487(15)	0.160079(11)	0.159612(14)
1000	0.160293(21)	0.160017(16)	0.159644(24)
2000	0.160162(22)	0.159910(15)	0.159691(27)
4000	0.160067(22)	0.159917(17)	0.159753(23)
8000	0.160060(27)	0.159888(19)	0.159759(26)
A_{gH}			
100	1.246920(42)	1.253683(42)	1.263604(39)
250	1.348559(45)	1.354758(52)	1.363108(43)
500	1.404691(68)	1.410316(71)	1.417575(62)
1000	1.44766(10)	1.452355(91)	1.458507(99)
2000	1.48008(15)	1.48402(15)	1.48946(16)
4000	1.50436(23)	1.50827(22)	1.51251(20)
8000	1.52336(30)	1.52607(32)	1.52933(32)

TABLE II. Estimates of the coefficients $S_{1,g}$ and $S_{2,g}$ for the radius of gyration.

N	$w = 0.375$	$w = 0.505838$	$w = 0.775$
$S_{1,g}$			
100	$-0.28885(58)$	$-0.30737(43)$	$-0.32464(55)$
250	$-0.30149(57)$	$-0.31331(46)$	$-0.32331(45)$
500	$-0.30663(71)$	$-0.31391(45)$	$-0.32202(65)$
1000	$-0.3093(10)$	$-0.31533(72)$	$-0.3184(11)$
2000	$-0.3121(11)$	$-0.31562(74)$	$-0.3183(10)$
4000	$-0.3105(11)$	$-0.31412(77)$	$-0.3161(13)$
8000	$-0.3144(13)$	$-0.31629(87)$	$-0.3166(14)$
$S_{2,g}$			
100	$-0.0451(49)$	$-0.0783(45)$	$-0.1324(55)$
250	$-0.0646(59)$	$-0.0905(48)$	$-0.1234(47)$
500	$-0.0752(65)$	$-0.0787(51)$	$-0.1190(72)$
1000	$-0.071(10)$	$-0.0950(73)$	$-0.082(11)$
2000	$-0.059(11)$	$-0.0920(78)$	$-0.105(10)$
4000	$-0.079(11)$	$-0.0883(81)$	$-0.080(13)$
8000	$-0.099(11)$	$-0.0896(89)$	$-0.080(12)$

TABLE III. Estimates of the coefficients $S_{1,e}$ and $S_{2,e}$ for the end-to-end distance.

N	$w = 0.375$	$w = 0.505838$	$w = 0.775$
$S_{1,e}$			
100	$-0.35414(79)$	$-0.37943(55)$	$-0.40439(68)$
250	$-0.36735(78)$	$-0.38421(58)$	$-0.39891(56)$
500	$-0.37364(85)$	$-0.38442(56)$	$-0.39570(91)$
1000	$-0.3780(13)$	$-0.38556(85)$	$-0.3911(11)$
2000	$-0.3814(13)$	$-0.38608(91)$	$-0.3891(13)$
4000	$-0.3801(13)$	$-0.38397(92)$	$-0.3866(14)$
8000	$-0.3848(16)$	$-0.38609(97)$	$-0.3878(16)$
$S_{2,e}$			
100	$0.0050(67)$	$-0.0271(62)$	$-0.0862(86)$
250	$-0.0058(86)$	$-0.0364(59)$	$-0.0694(65)$
500	$-0.0139(82)$	$-0.0225(69)$	$-0.062(10)$
1000	$-0.009(13)$	$-0.040(10)$	$-0.025(13)$
2000	$-0.006(15)$	$-0.042(10)$	$-0.038(14)$
4000	$-0.040(14)$	$-0.018(10)$	$-0.008(14)$
8000	$-0.039(16)$	$-0.035(11)$	$-0.025(14)$

TABLE IV. Estimates of the coefficients $S_{1,H}$ and $S_{2,H}$ for the hydrodynamic radius.

N	$w = 0.375$	$w = 0.505838$	$w = 0.775$
$S_{1,H}$			
100	0.09295(19)	0.09747(18)	0.10014(19)
250	0.09239(20)	0.09491(21)	0.09578(20)
500	0.09121(25)	0.09221(28)	0.09313(20)
1000	0.08991(39)	0.09031(40)	0.09097(34)
2000	0.08739(48)	0.08874(53)	0.08768(50)
4000	0.08708(68)	0.08822(53)	0.08747(59)
8000	0.08631(84)	0.08612(73)	0.08564(69)
$S_{2,H}$			
100	0.0668(19)	0.0851(21)	0.0999(24)
250	0.0731(23)	0.0826(22)	0.0967(23)
500	0.0782(30)	0.0822(27)	0.0902(29)
1000	0.0811(42)	0.0792(40)	0.0929(41)
2000	0.0730(50)	0.0911(62)	0.0747(62)
4000	0.0842(78)	0.0819(72)	0.0748(81)
8000	0.0773(97)	0.0738(94)	0.058(10)

TABLE V. Fit results for several values of N_{\min} .

	$N_{\min} = 100$	$N_{\min} = 250$	$N_{\min} = 500$	$N_{\min} = 1000$
A_{ge}^*	0.15991(4)	0.15989(4)	0.15988(4)	0.15995(7)
A_{gH}^*	1.5831(4)	1.5819(4)	1.5811(7)	1.5806(13)
$S_{1,g}^*$	-0.3144(8)	-0.3150(10)	-0.3152(15)	-0.3165(30)
$S_{2,g}^*$	-0.082(6)	-0.090(9)	-0.093(15)	-0.095(27)
$S_{1,e}^*$	-0.3846(9)	-0.3851(11)	-0.3851(18)	-0.3873(36)
$S_{2,e}^*$	-0.023(8)	-0.031(12)	-0.032(19)	-0.036(36)
$S_{1,H}^*$	0.0809(7)	0.0815(10)	0.0821(18)	0.0866(36)
$S_{2,H}^*$	0.068(7)	0.059(12)	0.044(22)	0.050(44)

TABLE VI. Estimates of the density corrections to R_g and R_e . Combined fits with data for A_{ge} .

	$N_{\min} = 100$	$N_{\min} = 250$	$N_{\min} = 500$	$N_{\min} = 1000$
$S_{1,g}^*$	-0.3149(9)	-0.3151(6)	-0.3152(7)	-0.3143(13)
$S_{2,g}^*$	-0.087(5)	-0.086(4)	-0.087(5)	-0.087(9)
$S_{1,e}^*$	-0.3846(13)	-0.3852(8)	-0.3853(7)	-0.3843(14)
$S_{2,e}^*$	-0.028(8)	-0.027(5)	-0.027(6)	-0.034(15)

FIGURES

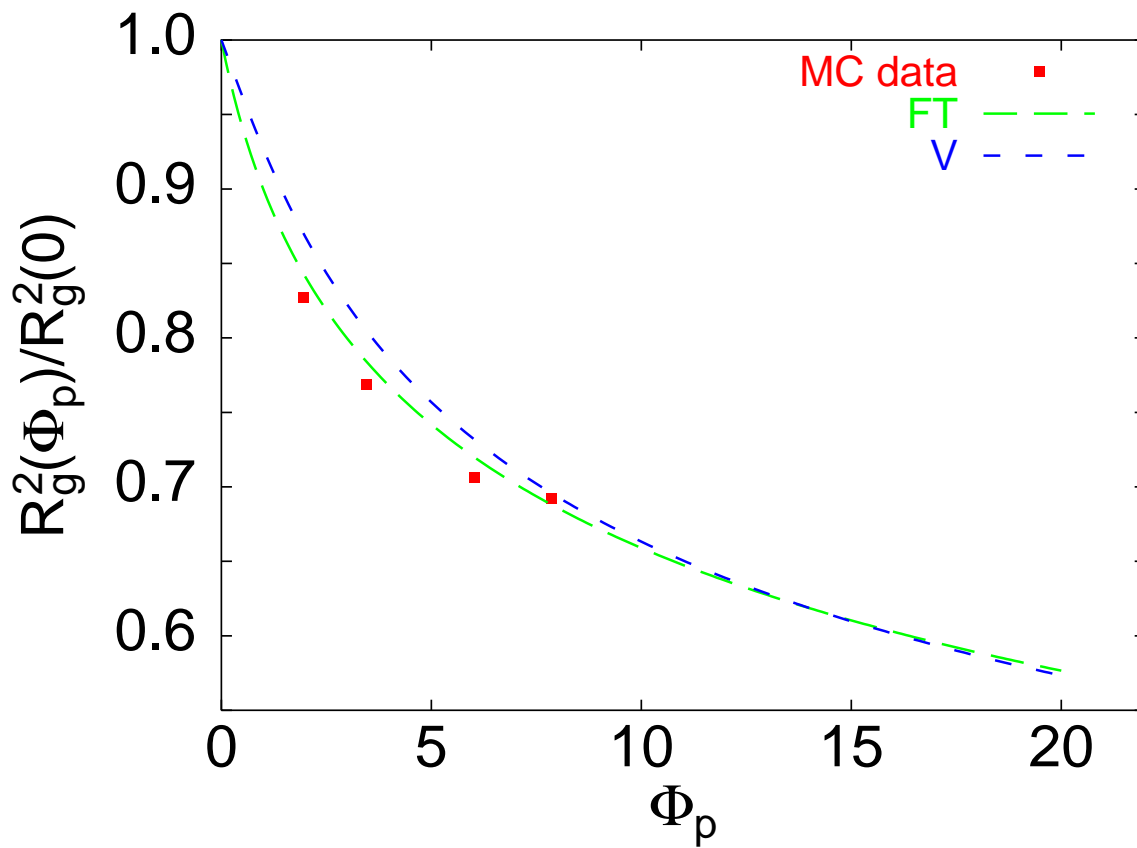


FIG. 1. Plot of R_g^2/\hat{R}_g^2 versus Φ_p . We report expression (5.7), “V”, the field-theoretical prediction of Ref. 25, “FT”, and the Monte Carlo data of Ref. 28.